Received: 25 June 2021 | Revised: 9 December 2021 | Accepted: 10 December 2021

DOI: 10.1002/glia.24131

GLIA

WILEY

RESEARCH ARTICLE

Contribution of astrocytes to familial risk and clinical manifestation of schizophrenia

Marja Koskuvi[1,2] | Šárka Lehtonen[1,2] | Kalevi Trontti[1,3,4] | Meike Keuters[1,2] | Ying-Chieh Wu[1] | Hennariikka Koivisto[2] | Anastasia Ludwig[1] | Lidiia Plotnikova[2] | Pekka L. J. Virtanen[1] | Noora Räsänen[1] | Satu Kaipainen[2] | Ida Hyötyläinen[2] | Hiramani Dhungana[1,2] | Raisa Giniatullina[2] | Ilkka Ojansuu[5] | Olli Vaurio[5] | Tyrone D. Cannon[6] | Jouko Lönnqvist[7,8] | Sebastian Therman[7] | Jaana Suvisaari[7] | Jaakko Kaprio[9] | Markku Lähteenvuo[5] | Jussi Tohka[2] | Rashid Giniatullin[2] | Claudio Rivera[1,10] | Iiris Hovatta[1,3,4] | Heikki Tanila[2] | Jari Tiihonen[1,5,11] | Jari Koistinaho[1,2]

[1]Neuroscience Center, University of Helsinki, Helsinki, Finland

[2]A.I. Virtanen Institute for Molecular Sciences, University of Eastern Finland, Kuopio, Finland

[3]SleepWell Research Program, Faculty of Medicine, University of Helsinki, Helsinki, Finland

[4]Department of Psychology and Logopedics, University of Helsinki, Helsinki, Finland

[5]Department of Forensic Psychiatry, University of Eastern Finland, Niuvanniemi Hospital, Kuopio, Finland

[6]Department of Psychology and Psychiatry, Yale University, New Haven, Connecticut, USA

[7]Mental Health Unit, Department of Public Health Solutions, National Institute for Health and Welfare, Helsinki, Finland

[8]Department of Psychiatry, University of Helsinki, Helsinki, Finland

[9]Institute for Molecular Medicine FIMM, University of Helsinki, Helsinki, Finland

[10]INSERM, Institute of Mediterranean Neurobiology, Aix-Marseille University, Marseille, France

[11]Department of Clinical Neuroscience, Karolinska Institutet, and Center for Psychiatric Research, Stockholm City Council, Stockholm, Sweden

Correspondence
Jari Tiihonen, Šárka Lehtonen and Jari Koistinaho, Neuroscience Center, University of Helsinki, Helsinki, Finland.
Email: jari.tiihonen@ki.se, sarka.lehtonen@uef.fi, and jari.koistinaho@helsinki.fi

Funding information
Academy of Finland, Grant/Award Numbers: A334525, AK 266820, AK 312073, AK 332354; Biocenter Finland; Business Finland; French National Agency for Research, Grant/Award Number: Acrobat; Sigrid Juselius Foundation; Orion Research Foundation;

Abstract

Previous studies have implicated several brain cell types in schizophrenia (SCZ), but the genetic impact of astrocytes is unknown. Considering their high complexity in humans, astrocytes are likely key determinants of neurodevelopmental diseases, such as SCZ. Human induced pluripotent stem cell (hiPSC)-derived astrocytes differentiated from five monozygotic twin pairs discordant for SCZ and five healthy subjects were studied for alterations related to high genetic risk and clinical manifestation of SCZ in astrocyte transcriptomics, neuron-astrocyte co-cultures, and in humanized mice. We found gene expression and signaling pathway alterations related to synaptic

We thank Marthe Van de Vliet, Eila Korhonen, Laila Kaskela, Sara Wojciechowski, Mirka Tikkanen and Velta Keksa-Goldsteine for technical help in generation and characterization of the stem cell lines. Biocenter Finland supported generation of iPSC lines.

Päijät-Häme Regional Fund Instrumentarium Science Foundation

dysfunction, inflammation, and extracellular matrix components in SCZ astrocytes, and demyelination in SCZ astrocyte transplanted mice. While Ingenuity Pathway Analysis identified SCZ disease and synaptic transmission pathway changes in SCZ astrocytes, the most consistent findings were related to collagen and cell adhesion associated pathways. Neuronal responses to glutamate and GABA differed between astrocytes from control persons, affected twins, and their unaffected co-twins and were normalized by clozapine treatment. SCZ astrocyte cell transplantation to the mouse forebrain caused gene expression changes in synaptic dysfunction and inflammation pathways of mouse brain cells and resulted in behavioral changes in cognitive and olfactory functions. Differentially expressed transcriptomes and signaling pathways related to synaptic functions, inflammation, and especially collagen and glycoprotein 6 pathways indicate abnormal extracellular matrix composition in the brain as one of the key characteristics in the etiology of SCZ.

KEYWORDS

calcium imaging, cell transplantation, extracellular matrix, induced pluripotent stem cells, monozygotic twins, RNA sequencing

1 | INTRODUCTION

Neuropharmacological studies have implicated abnormal dopaminergic, glutamatergic, and GABAergic activity in schizophrenia (SCZ) (Javitt et al., 2008), although the molecular mechanisms underlying the disease remain unclear. According to the current mainstream theory of the development of the disorder, genetic predisposition to SCZ is pronounced during embryonal development, and environmental effects trigger the symptoms in early adolescence (Davis et al., 2016). For example, early brain immune activation, such as upon exposure to maternal influenza, has long been known to increase susceptibility to SCZ (Khandaker et al., 2015). As postmortem studies can only reveal findings related to full-blown illness treated with antipsychotics, more information is needed about molecular changes at the early stage of the disease and before the psychosis in order to target prevention and early treatment for people in high-risk groups. Several SCZ-associated genes are involved in the development and physiology of glial cells (González-Peñas et al., 2019; Toker et al., 2018). Therefore, the importance of astrocytes in neurodevelopmental diseases has gained more interest. Because of their key roles in maintaining CNS homeostasis, synapse formation and the synaptic metabolism of glutamate and monoamines, astrocyte dysfunction may lead to abnormal neurotransmitter release in SCZ (Wang et al., 2015).

Human induced pluripotent stem cell (hiPSC) models have been used to explore neuropathological abnormalities in patients with SCZ, but so far, the main focus has been on neuronal pathophysiology, while the contribution of astrocytes has received much less attention. One study using hiPSC-derived astrocytes obtained from patients with SCZ showed impaired astrocyte maturation related to enhanced BMP signaling pathway in childhood-onset patients with SCZ (Liu et al., 2019). Another study found attenuated C-C Motif Chemokine Ligand 20 (CCL20) response and T cell recruitment in patients with SCZ after Interleukin-1β (IL-1β) exposure (Akkouh et al., 2020). Moreover, transplanted human iPSC-derived glial progenitors obtained from childhood-onset SCZ patients have shown delayed astrocytic differentiation and abnormal astrocyte morphologies, as well as behavioral abnormalities in mouse brains (Windrem et al., 2017).

We previously generated hiPSCs from five monozygotic twin pairs discordant for SCZ and five healthy controls. We showed sex-specific differences in gene expression of hiPSC-derived cortical neurons, especially in pathways associated with N-glycan synthesis, CAMK2G, GABAergic synapse, and purine metabolism in SCZ (Tiihonen et al., 2019), which are largely in line with previous literature on molecular mechanisms of SCZ. In this study, we differentiated hiPSCs from the same twin pairs and healthy controls into astrocytes. We hypothesized that gene expression profiling of astrocytes may reveal molecules and pathways that are associated with increased genetic risk for SCZ (between all twins and healthy controls) and clinical manifestation of the illness (between affected twins (ST) and unaffected twins (HT)). Because men and women are known to have different types of lifespan calendars of gene expression, and the phenotype, age of onset, and antipsychotic responses in SCZ are sex-dependent (Li et al., 2016; Skene et al., 2017), we further hypothesized that similar to iPSC-derived neurons (Tiihonen et al., 2019) also iPSC-derived astrocytes show at least trends towards sexual dimorphism at the transcriptional level. To verify possible functional consequences on neuronal and brain functions, we investigated whether astrocytes from patients with SCZ dysregulate neuronal calcium responses in neurons or alter brain endogenous gene expression upon astrocyte engraftment into neonatal mouse brain.

2 | MATERIALS AND METHODS

2.1 | Patient iPSC-lines and astrocyte differentiation

The Ethics Committee of the Helsinki University Hospital District approved this project. Five monozygotic twin pairs discordant for SZ and five age and sex-matched healthy volunteers were included. The patients' description and characterization of the iPSC lines are published in Tiihonen et al. (2019). The hiPSC-derived astrocytes were differentiated using the previously published protocol (Krencik & Zhang, 2011; Oksanen et al., 2017) with slight modifications described in Supplementary Methods. The differentiated astrocytes show functions, responses to stimuli, marker and gene expression typical to astrocytes (Oksanen et al., 2017, 2019).

2.2 | RNA isolation and sequencing

Extraction and purification of the RNA from cultured hiPSC-derived astrocytes and transplanted mouse tissues are described in Supplementary Methods. RNA-sequencing libraries were produced from hiPSC-derived astrocytes of ST, HT, and Ctrl (all groups $n = 5$; 2 males and 3 females), and cortices of mice transplanted with hiPSC-derived astrocytes from ST, HT or Ctrl subjects (altogether 18 cortices; $n = 6$ mice/group), and control cortices ($n = 3$) without transplantation. The preparations of RNA sequencing libraries read alignment strategies, qRT-PCR, and mouse studies have been described in Supplementary Methods.

2.3 | Calcium imaging and analysis

hiPSC-derived neuron and astrocyte co-cultures were loaded with Fluo-4 followed by sequential 2-min neuron stimulation with glutamate together with NMDA receptor co-agonist glycine, GABA, and KCl. The recordings performed with an inverted ZEISS Axio Observer microscope equipped with Prime BSI sCMOS camera were analyzed blinded using a custom script in MatLab software. Mean pixel intensity of masked regions of interests corresponding to individual cells was measured at each time point. Traces were detrended, and the intensity of the treatment period was normalized to the baseline intensity to produce $\Delta F/F$. A detailed description is in Supplementary Methods.

2.4 | Transplantation

hiPSC-astrocyte progenitors (100,000 cells/μl in PBS) dissociated from sphere cultures with Accutase (Stemcell technologies) from two female twin pairs and two female controls were transplanted into newborn Rag1 knockout mouse (B6.12957-Rag1tm1Mom/J, The Jackson Laboratory) forebrain using the protocol published by Kim et al., 2014. A detailed description of animal handling and behavior tests are in Supplementary Methods.

2.5 | Data availability

Supplementary Data files show raw RNA seq data. All the calcium imaging analysis codes were written in Matlab and are available on request from the authors. The detailed data of mouse behavioral studies are available on request from the authors. The RNA sequencing data is also available in GEO: GSE191250.

3 | RESULTS

3.1 | SCZ and control hiPSCs differentiate evenly to astrocytes with similar cell-specific properties

The five adult SCZ-discordant monozygotic twin pairs and five unrelated healthy control (Ctrl) hiPSC-lines have been fully characterized before (Supplementary Table 1) (Tiihonen et al., 2019). No significant differences were found between the groups or lines in differentiation efficiency based on protein or RNA expression levels of astrocyte-specific markers or glucose and glutamate uptake (Figure 1a, Supplementary Figure 1).

3.2 | SCZ astrocytes show changes suggesting sex-specific gene expression alterations

We assessed whether gene expression profiles associated with familial risk or clinical illness of SCZ in hiPSC-derived astrocytes are suggestive for sex-specific changes using transcriptomic analysis. Figure 1b summarizes the number of differentially expressed genes (DEGs; Benjamini–Hochberg corrected p-value < .05 and absolute log2-fold change >1.0) in comparisons between ST and Ctrl (associated with both familial risk and clinical illness), HT and Ctrl (associated with familial risk without clinical illness), ST and HT (associated with pure clinical illness), and between all twins and Ctrl (associated with familial risk with or without clinical illness) of all participants and when separated by sex. The number of DEGs increased from tens to hundreds in all comparisons when the sexes were analyzed separately and were far more numerous in males than females. To determine whether astrocytes might contribute to sex differences in SCZ, we compared the number of sex-specific gene expression differences between SCZ and Ctrl astrocytes. First, 1.3% of genes (8461/34,783) were expressed differentially in female versus male Ctrl astrocytes. Before separating the sexes, the proportion of sex-specific genes reached up to 22.6% of the DEGs (ST vs. HT, $p = 1.32 \times 10^{-25}$), and after the separation, the proportion was up to 47.0% (Female HT vs. Ctrl, $p < 2.23 \times 10^{-308}$).

The lists of DEGs are found in Supplementary Data 1–12, and the 20 most significant DEGs in the ST versus HT comparison with combined sexes, females (all DEGs), and males, are shown in Figure 1c. In the ST versus Ctrl comparison, top genes such as *CHL1*, *CNTN1*, *CDH8*, *CDH13*, and *PCDHGB7*, related to cell

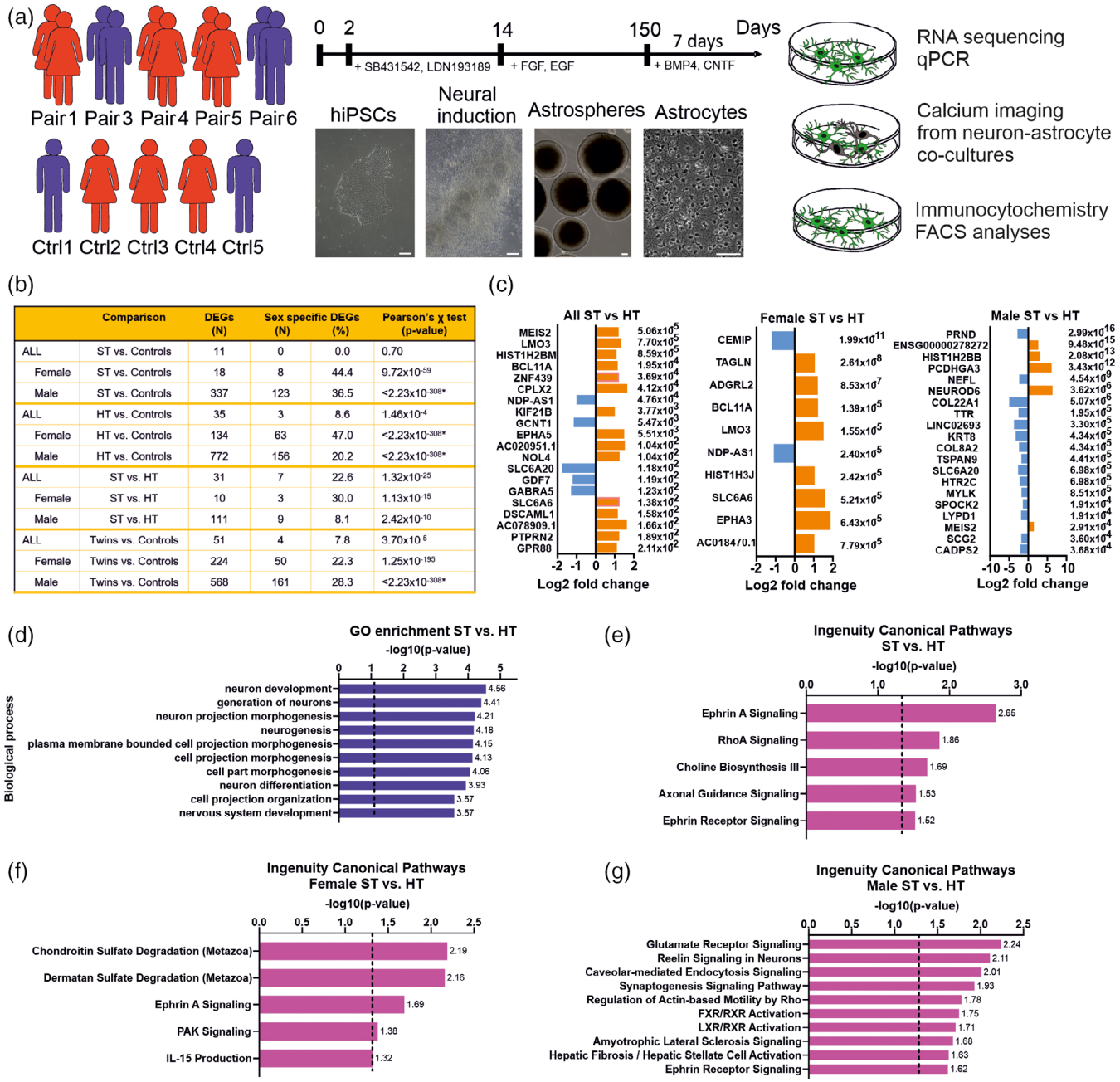

(b)

	Comparison	DEGs (N)	Sex specific DEGs (N)	Sex specific DEGs (%)	Pearson's χ test (p-value)
ALL	ST vs. Controls	11	0	0.0	0.70
Female	ST vs. Controls	18	8	44.4	9.72×10^{-59}
Male	ST vs. Controls	337	123	36.5	$<2.23 \times 10^{-308*}$
ALL	HT vs. Controls	35	3	8.6	1.46×10^{-4}
Female	HT vs. Controls	134	63	47.0	$<2.23 \times 10^{-308*}$
Male	HT vs. Controls	772	156	20.2	$<2.23 \times 10^{-308*}$
ALL	ST vs. HT	31	7	22.6	1.32×10^{-25}
Female	ST vs. HT	10	3	30.0	1.13×10^{-15}
Male	ST vs. HT	111	9	8.1	2.42×10^{-10}
ALL	Twins vs. Controls	51	4	7.8	3.70×10^{-5}
Female	Twins vs. Controls	224	50	22.3	1.25×10^{-195}
Male	Twins vs. Controls	568	161	28.3	$<2.23 \times 10^{-308*}$

FIGURE 1 RNA expression analysis of ST and HT twins using hiPSC-derived astrocytes. (a) The summary of the differentiation of hiPSCs derived from twin pairs discordant to SCZ (red, female; blue, male) and controls towards astrocytes. Scale bar 50 μm. (b) The comparison table of differentially expressed genes (DEGs) and proportion of sex-specific DEGs in comparison sets (cutoffs: Adjusted *p*-value <.05 and absolute log2 fold change >1.0). The *p*-value for sex-difference was too small to count in the used platform in four comparisons, which reached to 2.23×10^{-308}. (c) The 20 most significant DEGs in ST versus HT comparisons with both sexes, females and males. (d) the most significant GO enrichment terms in ST versus HT and IPA pathways in ST versus HT with (e) both sexes, (f) females, and (g) males. Dash line is value for $p = .05$. Abbreviations: Ctrl, control, ST, affected twin, HT, unaffected co-twin

adhesion, were expressed among both males and females. *CHL1* was the number one top gene also in the male ST versus Ctrl (adjusted $p = 9.6 \times 10^{-75}$) and male HT versus Ctrl comparison (adjusted $p = 5.1 \times 10^{-93}$). In the HT versus Ctrl comparison, the DEGs included downregulation of *SHISA6* (−2.6 log2 fold change, adj. $p < .05$).

3.3 | Pathways related to neuronal wiring and inflammation are altered in SCZ astrocytes

Total numbers of Gene Oncology (GO) terms (Benjamini-Hochberg, adj. $p < .05$) and Ingenuity Pathway Analysis (IPA) pathways (−log(*p*-value) > 1.3) in each comparison are listed in Supplementary Table 2

and the lists of GO terms in Supplementary Data 13–19 and IPA canonical pathways in Supplementary Data 20–28. In comparing ST and HT, 30 GO terms involving neuron development and generation of neurons were detected as the most significant terms (10 most significant GO terms in Figure 1d, all in Supplementary Data 18). In males, Glutamate Receptor Signaling ($-\log(p) = 2.24$) was the most significant pathway, and Ephrin receptor pathways were altered among both sexes (Figure 1f,g, Supplementary Data 27–28).

A strongly significant change appeared in Hepatic Fibrosis Signaling, which was found in the male ST versus HT comparison, male ST versus Ctrl and HT versus Ctrl comparisons, and in the female HT versus Ctrl comparison. This pathway is prominently induced by experimental inflammation in astrocytes (Cao et al., 2019) and shares several genes related to extracellular matrix (ECM) and adhesion with Glycoprotein 6 (GP6) pathway, which was detected in the male ST versus HT ($-\log(p) = 1.54$), ST versus Ctrl (3.97) and HT versus Ctrl (6.47) comparisons.

The pathway analysis of the HT versus Ctrl comparison in females revealed Synaptogenesis Signaling, Ephrin Receptor, and IL-15 Production pathways in addition to Hepatic Fibrosis/Hepatic Stellate Cell Activation pathway (Supplementary Data 24), whereas, in males Wnt, Synaptogenesis, Ephrin, and inflammation-related pathways were identified (Supplementary Data 25).

3.4 | The synaptic transmission associated altered gene sets in SCZ astrocytes appear to be distinct in males and females

>IPA function and disease pathways in ST versus HT comparison identified neuronal exocytosis and postsynaptic excitatory processes (Figure 2a–c). Importantly, SCZ disease pathway appeared among the most significant pathways in each male comparison ($p = 2.14 \times 10^{-6}$–1.18×10^{-7}) (Figure 2d) and was also significant in female twins versus Ctrl ($p = 6.93 \times 10^{-4}$) comparison. Many of the genes contributing to the SCZ disease pathway were related to neurotransmitters and synaptic transmission. Thus, the functional pathway for synaptic transmission also appeared significant in separate sex comparisons (Figure 2e). In Synaptic transmission pathway, IPA predicted high decrease for the female Twins versus Ctrl (z-score $= -2.4$, p-value $= 1.6 \times 10^{-6}$), but an equally high increase for the male Twins versus Ctrl ($z = 2.1$, $p = 5.1 \times 10^{-6}$), respectively. Among the shared genes with the opposite direction of expression were genes previously associated with SCZ: *RAPGEF4*, *GRIK2*, *CNTNAP2*, and *CDH8* (Figure 2f–g: females, h–i: males).

3.5 | Altered pathways in our comparisons were comparable to the hiPSC-GPC data set with patients with childhood-onset SCZ

For comparison, we performed IPA analysis from DEGs generated in the Windrem et al. (2017) data (116 DEGs in glial progenitor cells derived from patients with childhood-onset SCZ, absolute log2fold change >1.0, FDR 5%, Supplementary Data 29). The first two pathways (Glutamate Receptor Signaling ($-\log(p) = 4.06$) and Amyotrophic Lateral Sclerosis Signaling (3.17)), and Synaptogenesis Signaling Pathway (1.41) were shared with our male ST versus HT comparison (Supplementary Figure 2a and Supplementary Data 30). The Synaptic transmission pathway was significant ($p = 1.06 \times 10^{-9}$) with 15 genes. Four genes in four comparisons were shared with the Windrem data set (Supplementary Table 3).

3.6 | SCZ astrocytes modulate neurotransmitter responses

Responses to glutamate and GABA in hiPSC-neurons as Ca^{2+} influx were recorded from healthy female hiPSC-cortical neurons co-cultured with hiPSC-astrocytes from ST, HT, and Ctrl persons (Figure 3a,b, Supplementary Figure 3). When the effect of twins' astrocytes was compared to same-sex Ctrl astrocytes, no differences were detected in glutamate response between HT and Ctrl. In contrast, neurons co-cultured with ST astrocytes of either sex showed an increased response to glutamate (adj. $p < .0001$) compared to co-cultures with HT or Ctrl astrocytes (Figure 3c,d, Supplementary Tables 4–5). While neurons with male ST or female HT astrocytes showed increased Ca^{2+} response after GABA treatment (adj. $p < .0001$). The proportions of responding neurons were the same between the astrocyte groups (Supplementary Figure 3c–d).

After clozapine application, the increased Ca^{2+} response to glutamate observed in neurons co-cultured with ST astrocytes decreased (adj. $p < .0001$) to Ctrl level in both the males and females. Similarly, the Ca^{2+} response to GABA decreased in clozapine-treated cells, but was insufficient in male ST (adj. $p < .0001$) and HT (adj. $p < .01$), and in female HT (adj. $p < .05$) astrocyte co-cultured neurons.

3.7 | Transplanted hiPSC-astrocyte progenitors mature into astrocytes and induce subtle behavioral changes

Because from the patients from which the iPSC lines were generated, the females had more severe symptoms than males, we transplanted female ST, HT, and Ctrl hiPSC-astrocyte progenitors into neonatal mouse forebrains and analyzed mouse behavior at 5 and 10 months, followed by gene expression profiling of the frontal cortices 7 days later (Figure 4, Supplementary Figure 4). A behavioral test battery covering motor, sensory, emotional, social and cognitive functions relevant for SCZ was used (for more details, see Methods in Supplementary information). In a Novel Object Recognition test, experimental objects caused high stress, so that 38.1% of ST mice compared to 12.5% and 22.2% of Ctrl and HT mice, respectively, were disqualified from the test at 5 months (Supplementary Table 6). For the remaining mice, the test showed a significant age × transplantation interaction ($p = .02$, General linear model, repeated measures), such that ST

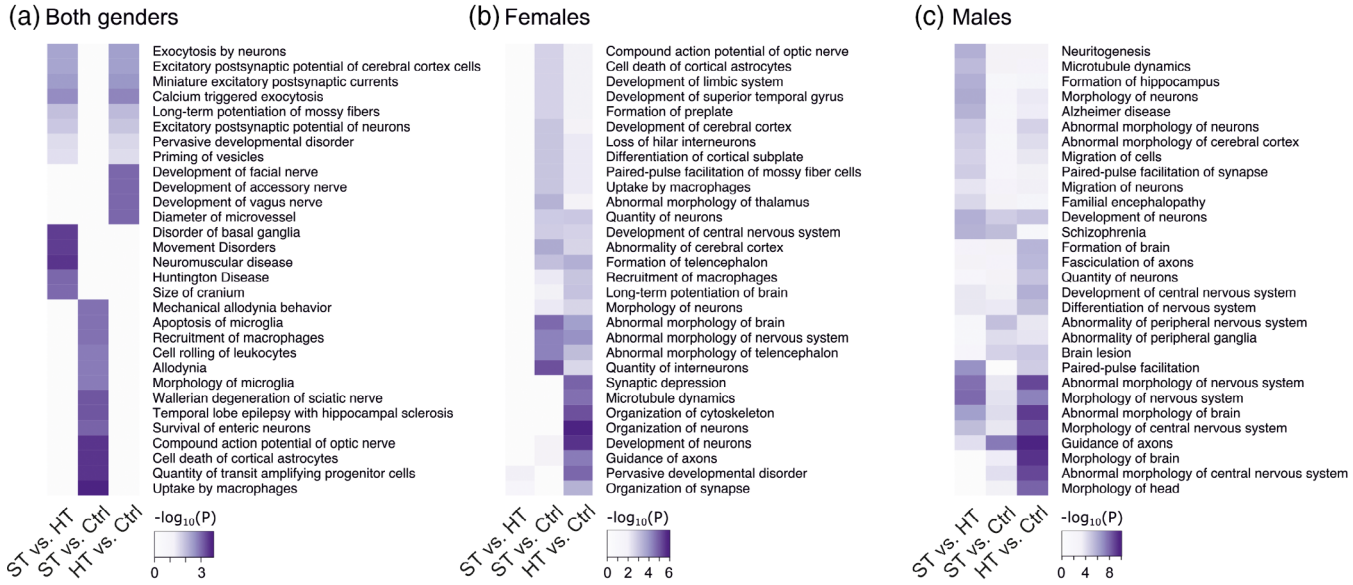

(d) Schizophrenia

		p-value	Molecules in pathway
ST vs. HT	All	n.s.	
	Female	n.s.	
	Male	2.14×10^{-6}	DAAM2,GRIN2A,STMN2,SCG2,CNR1,HTR2C,CALB1,GRIK3,NEFL,TTR
ST vs. Ctrl	All	n.s.	
	Female	n.s.	
	Male	1.18×10^{-7}	ADRB2, CXCL12, CMYA5, LGALS1, ACTA2, PCSK1, NBPF1(includes others), IFITM3, GRM3, CA2, CA12, PRKCB, SLC1A3, GRIK3, NTF3, GABRB2, NRG1, ZNF492/ZNF98, SCN1A, STMN2, ZNF804A, SEMA3A, GAD2, CA3, HTR2C, TTR
HT vs. Ctrl	All	n.s.	
	Female	n.s.	
	Male	1.64×10^{-7}	ADRB2 CXCL12, GAD1, COMT, CMYA5, IL6R, RTN2, ACTA2, PCSK1, ATP1A2, NBPF1(includes others), IFITM3, TSPO, GRM3, CHI3L1, CRYM, KCNH7, CA4, GRM5, LAMA2, CSMD1, SCN2B, NTF3, NRG1, GABRQ, NRXN1, ZNF492/ZNF98, CTNNA2, CAV1, DAAM2, SCN1A, DPYD, CACNA2D1, SEMA3A, CA3, TRANK1, CADPS2, ALDOC, HTR2C, CALB1, RARG, CCKAR, SERPINI1, TTR
Twins vs. Ctrl	All	n.s.	
	Female	6.93×10^{-4}	PRDX6, ACHE, ROBO1, VGF, CACNA2D2, RGS4, PCLO, CUX2, RYR2, SERPINI1, HTR2A, NELL1
	Male	1.60×10^{-7}	ADRB2 CXCL12, COMT, CMYA5, IL6R, RTN2, ACTA2, PCSK1, ADRA1D, NBPF1(includes others), IFITM3, TSPO, GRM3, CHI3L1, SLC26A7, SCG5, SLC18A1, CA4, GRM5, LAMA2, SST, NTF3, NRG1, ZNF492/ZNF98, PTGIS, CTNNA2, SCN1A, DPYD, ZNF804A, SEMA3A, CA3, CADPS2, HTR2C, CCKAR, TTR

(e) Synaptic transmission

		p-value	z-score	Molecules in pathway (Genes of interest in bold)
ST vs. HT	All	n.s.	-	
	Female	n.s.	-	
	Male	1.23×10^{-5}	0.45	LGI1, PRNP, GRIN2A, CNR1, RIMS1, APOE, LYPD1, NRXN1
ST vs. Ctrl	All	n.s.	-	
	Female	3.68×10^{-4}	-	**GRIK2, CNTNAP2, CDH8**, KCNJ6
	Male	4.31×10^{-7}	-0.71	ADRB2, KCNMA1, SLC6A6, **RAPGEF4**, GRIA1, NPY2R, ALK, NTF3, GABRB2, KCNA1, GRM3, DLGAP1, KCNJ9, HLA-A, SCN1A, HAP1, PTK2B, PRKCB, GAD2, SLC1A3, PCDHB5
HT vs. Ctrl	All	n.s.	-	
	Female	1.38×10^{-7}	-1.26	SLC6A6, UNC13A, **GRIK2**, DPP6, EPHB2, EPHB1, LRP8, KCNJ6, RIMBP2, PTPRD, DGKB, SHANK2, **CNTNAP2**, KCNQ3
	Male	1.74×10^{-9}	1.79	ADRB2 LGI1, GAD1, WNT5A, NR3C2, NQO1, KCNA1, GRM3, NLGN1, KCND2, **CNTNAP2**, NRG3, GRM5, GRM8, ADCY8, PCDHB5, FGF12, SCN2B, TNFRSF1B, **RAPGEF4**, **GRIK2** NPY2R, ALK, RIMS1, NTF3, FBXO2, PLAT, NRXN1, CAMK2A, LYNX1, DLGAP1, HLA-A, CAV2, PMCH, SCN1A, GPR176, PCDHB16, APOE, LYPD1, **CDH8**
Twins vs. Ctrl	All	n.s.	-	
	Female	1.57×10^{-6}	-2.41	UNC13A, **RAPGEF4**, ERC2, **GRIK2**, CLSTN2, NBEA, KCNJ6, PTPRD, DGKB, SHANK2, **CNTNAP2**, LYPD1, **CDH8**, KCNQ3
	Male	5.08×10^{-6}	2.14	ADRB2, SLC6A6, WNT5A, KCNA1, GRM3, KCNJ9, KCND2, **CNTNAP2**, GRM5, ADCY8, PCDHB5, SST, KCNMA1, TNFRSF1B, **RAPGEF4**, **GRIK2**, NPY2R, ALK, NTF3, CAMK2A, DLGAP1, HLA-A, PMCH, SCN1A, PCDHB16, **CDH8**

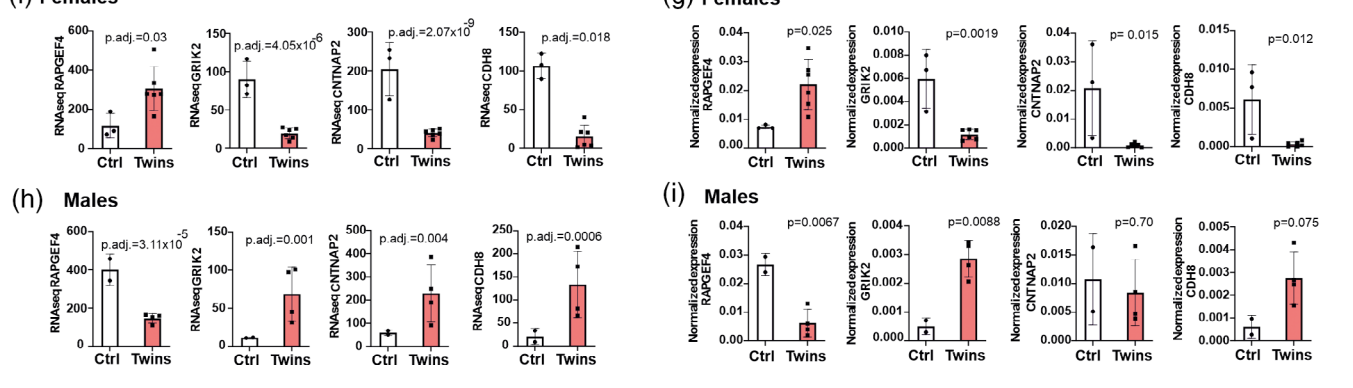

FIGURE 2 Ingenuity pathway analysis of disease and function pathways. The 30 disease and function pathways with the highest *p*-value in different comparisons among (a) all, (b) female, and (c) male groups. (d) Schizophrenia disease pathway and related molecules in the pathway in different comparisons. (e) Synaptic transmission function pathway and related molecules in the pathway in different comparisons. RNA sequence expression of the genes of interest in (f) females and (g) their validation by RT-qPCR and (h) in males and (i) their validation. (f) and (h) have Benjamini–Hochberg corrected *p*-value, and (g) and (i) have nominal *p*-value calculated by unpaired *t*-test. The data is presented as mean ± SD. Abbreviations: Ctrl, control, ST, affected twin, HT, unaffected co-twin

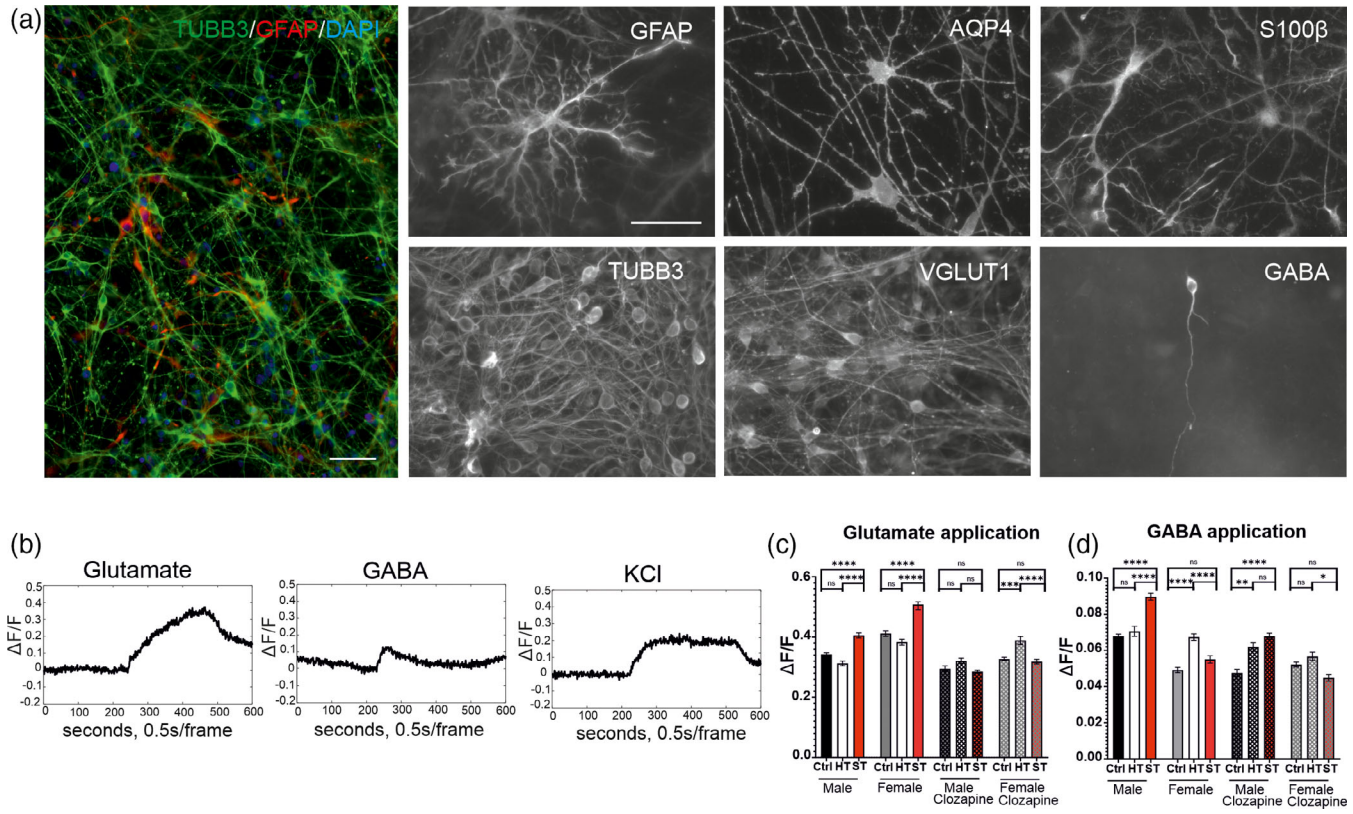

FIGURE 3 Calcium imaging of control neurons co-cultured with astrocytes. (a) co-cultured astrocytes expressed *GFAP* (red) and neurons *TUBB3* (green). Astrocytes showed a typical stellate morphology and *AQP4* and *S100β* expression. *TUBB3*$^{+}$ neuronal cells were positive to *VGLUT1* or *GABA*. The scale bar is 50 μm. (b) Examples of calcium traces in neuronal KCl^{+} cells after application of glutamate with glycine, GABA and KCl. Neuronal responses were presented as Δ*F*/*F* values from **c** glutamate and (d) GABA applications. Each group has pooled ΔF/F values from cells from 2 to 3 subjects, 4–6 recordings, 600–2700 cells per condition. The data is presented as mean ± SE. **** $p < .0001$, ***$p < .001$, ** $p < .01$, 3-way ANOVA and Tukey's post-hoc test. Abbreviations: Ctrl, control, ST, affected twin, HT, unaffected co-twin

mice had a preference for novelty as they aged. At the age of 10 months, ST mice showed the least preference (0%) for the odor of an unknown mouse compared to their own odor. In contrast, when exposed to cardamom and their own odor the day after, only ST mice demonstrated an equal preference for cardamom (novel but socially neutral odor) as their own odor (familiar but socially significant odor) (Figure 4b). The other behavior tests did not identify any differences between the groups (Supplementary Figure 5).

3.8 | Transplanted SCZ astrocytes induce synaptic dysfunction and inflammation pathways in mouse brain

The humanized mice's frontal cortical tissues were used for transcriptomic analysis, as this brain area shows early involvement in SCZ pathophysiology (Selemon & Zecevic, 2015). Based on human-specific immunostainings (Figure 4e, Supplementary Figure 4) and RNA expression profile of human-derived reads (Supplementary Figure 6b), the majority of the transplanted cells maturated to astrocytes. The transplanted human cells affected 872 individual mouse genes (adj. $p < .05$) and 225 mouse signaling pathways (Supplementary Figure 6f, Supplementary Tables 34 and 37) including Axonal Guidance ($-\log10(p) = 11.3$) and Synaptogenesis Signaling ($-\log10(p) = 9.21$) pathways. However, significantly less ST astrocytes than Ctrl or HT astrocytes migrated to mouse cortices based on the human cytoplasmic marker cell count. Similarly, the amount of ST-transplanted human reads was lower than in Ctrl- or HT-transplanted mice (Supplementary Figure 4d,e). Thus, we decided to look only at transcriptomic differences between HT and Ctrl animals. The analysis was done with mouse cell-derived reads (for more details, see Methods in Supplementary information, Supplementary Figure 6a,b, and Supplementary Data 31) using the threshold of .05 for nominal *p*-value as DEG criterion because none of the mouse DEGs survived Benjamini-Hochberg adjustment (Supplementary Table 7). Importantly, we detected Neuroinflammation Signaling Pathway ($-\log10(p) = 1.59$) (Supplementary Figure 6d,e, Supplementary Data 32 and 36) in HT mice versus Ctrl mice, and two pathways, Proline biosynthesis ($-\log10(p) = 3.09$) and Folate polyglutamylation ($-\log10(p) = 2.88$), associated with glutamate metabolism. Triacylglycerol degradation ($-\log10(p) = 2.66$) and Adipogenesis ($-\log10(p) = 2.30$) pathway were also among five the most significant pathways between HT and Ctrl mice. Interestingly, our HT mice

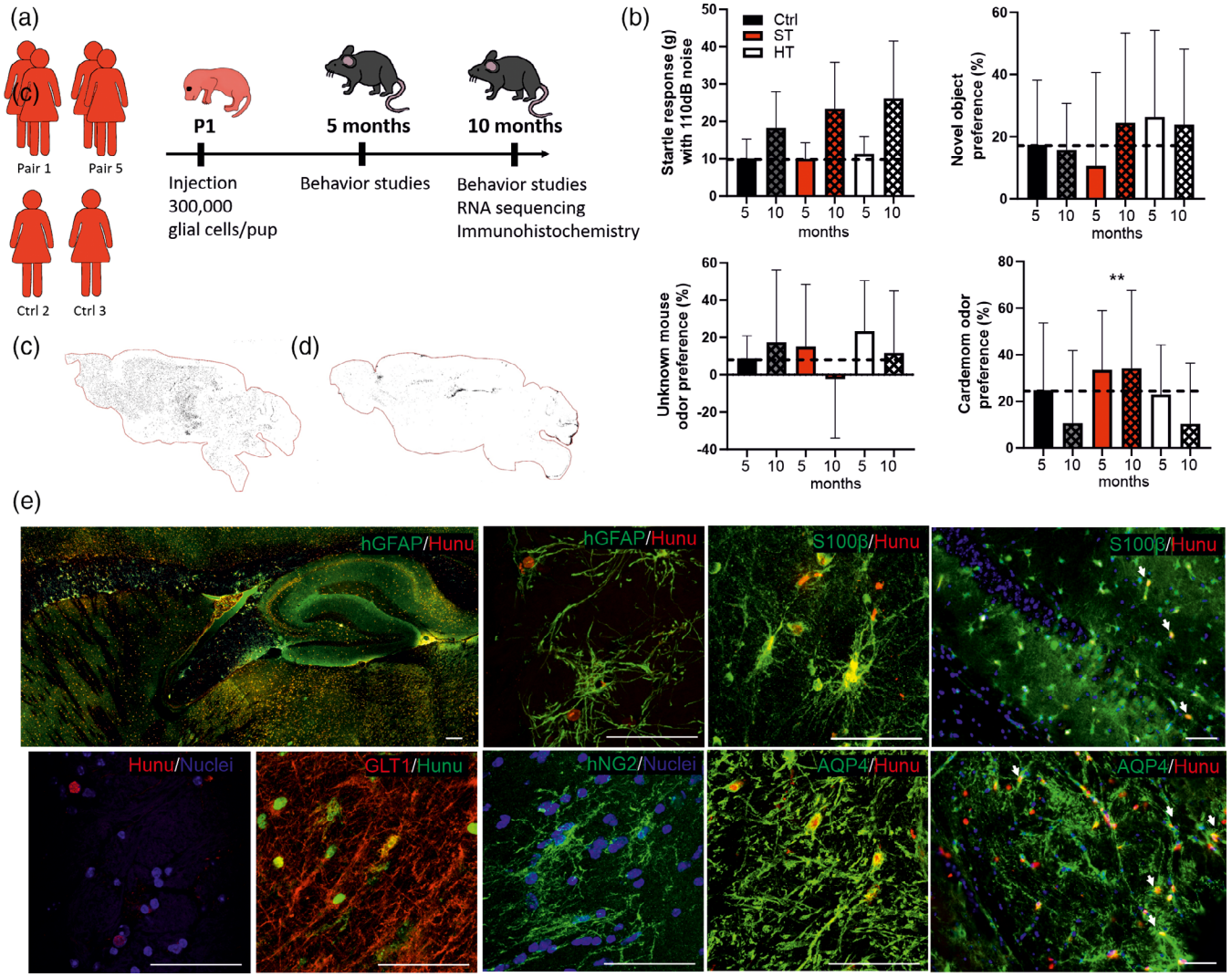

FIGURE 4 Transplantation of human astrocytes into neonatal mouse brain. (a) schematic illustration of hiPSC-glial progenitor chimeras that were established by neonatal injections into rag 1 KO hosts and sacrificed after 10 months. (b) results from behavioral studies: Prepulse inhibition, novel object preference, unknown mouse odor preference, and cardamom odor preference of the transplanted mice. Ctrl, $n = 16$, ST $n = 21$, and HT $n = 27$. The results are presented as mean ± SEM. ** $p < .01$, * $p < .05$. Representative pictures from *Hunu*$^+$ cells (human nuclei) and human *GFAP*+ cells. Sagittal sections demonstrating the distribution of (c) *Hunu* and (d) *GFAP*. (e) The representative images of human *GFAP*, *S100β*, human *NG2*, *GLT1*, *AQP4*, and *Hunu* (human nuclei). Scale bar in all 50 μm. Abbreviations: Ctrl, control, ST, affected twin, HT, unaffected co-twin

were significantly more obese at 10 months old than ST- or Ctrl-transplanted mice (Supplementary Figure 6c).

Even though different numbers of present human astrocytes would bias the comparison between Ctrl and ST animals, we looked side-by-side Ctrl versus non-transplant and ST versus non-transplant comparisons whether there are DEGs only related to ST-astrocyte transplantation. Between ST and non-transplanted we identified totally 553 DEGs (*p*.adj. <.05) (Supplementary Data 33). Once we compared the list of DEGs, there were DEGs which were only significantly expressed in ST versus non-transplant, but not in Ctrl versus non-transplant, for example, serotonin receptor Htr2a, and ECM molecules Cdh9 (Cadherin 9), Pcdh17 (Protocadherin 17), and Hspg2 (Heparan Sulfate Proteoglycan 2), and astrocytic channel protein Aqp4 (Aquaporin 4) (Supplementary Figure 6g, Supplementary Data 35, 38–39).

4 | DISCUSSION

Here, we generated hiPSC-astrocytes from monozygotic twins discordant for SCZ and controls to study transcriptional and functional changes. Concordance rate for both twins to develop SCZ is around 50% due to genetic or epigenetic factors (Cardno & Gottesman, 2000). The possible traces of epigenetic alterations after iPSC-reprogramming are completely outweighed by individual genetic variations and differentiation-associated changes (de Boni et al., 2018; Vitale et al., 2017). A substantial number of early developmental mutations specific for one of the monozygotic twins are frequent (Jonsson et al., 2021). As our previous CNV analysis identified 26 and 18 de novo mutations in only ST or HT twins, respectively (Tiihonen et al., 2019), the alterations in transcription between discordant twins may primarily be explained by early postzygotic mutations.

Our data showed aberrant expression of glutamatergic and GABAergic receptor genes in SCZ astrocytes. Especially *GRIK2* was sex-specifically expressed in astrocytes of affected and unaffected twins. Furthermore, affected twin astrocytes modulated healthy neuron calcium responses to glutamate and GABA in co-cultures. These data suggest that dysfunction of the glutamatergic or the GABAergic signaling contributing to neuronal excitatory/inhibitory imbalance in SCZ (Cherlyn et al., 2010) may at least in some SCZ cases be indirectly due to the dysfunction of these particular pathways in astrocytes.

One of the most significant findings in the behavior of ST-transplanted mice was their increased interest in cardamom odor, a novel but socially neutral odor, over their own odor. We interpret the finding with two factors: reduced social interest and enhanced odor sensitivity of the ST mice. We also noticed that the mice in HT group showed altered gene expression of fatty acid related pathways in the cortex by 10 months of age while gaining more weight when compared to other mouse groups. Metabolic syndrome is highly prevalent among patients with SCZ and potentially contributes to cognitive symptoms in SCZ (Hert et al., 2009). The reason for not detecting similar changes in fatty acid pathways and mouse weight could be due to limited amount of SCZ astrocytes in the mouse cortex.

Our identification of many differentially expressed adhesion and collagen genes in astrocytes between affected and unaffected twins and healthy individuals indicates the involvement of ECM in SCZ (Gray et al., 2015; Halassa et al., 2007). ECM is synthesized by both neural and glial cells and has both protective and suppressive effects (Song & Dityatev, 2018). Previous studies have implicated ECM in regulation of cell migration and neurite outgrowth (Tiihonen et al., 2021), and in perineuronal nets in protection of parvalbumin-expressing GABA interneurons (Berretta, 2012; Wen et al., 2018). After brain injuries, neuroinflammation, and neurodegeneration, particularly reactive astrocytes modify the brain ECM to build physiological and chemical barriers which inhibit axonal growth and reduce plasticity. Notably, astrocytic ECM is crucial in synapse formation and stabilization in brain development. We demonstrated strongly altered astrocyte expression of *CHL1*. *CHL1* regulating neuronal survival and growth and dendritic spine pruning in developing pyramidal neurons has been linked to SCZ in several studies (Mohan et al., 2019). It was also one of the most altered genes in the affected male twins versus healthy controls and unaffected twins versus healthy controls comparisons in hiPSC-derived neurons (Tiihonen et al., 2019). Abnormalities in collagen genes are associated with SCZ (Cao et al., 2019), and in animal models loss of certain collagen molecules results in decreased inhibitory synapse number, reduction in perineuronal nets and SCZ-related behaviors (Su et al., 2016, 2017). Taken together, we identified links between altered gene expression in inflammation, ECM, and synaptic pathways in astrocytes of individuals with clinical illness and familial risk, which are associated with altered regulation of neurotransmitter responses in neurons.

In conclusion, our results showed that signaling pathways related to inflammation, synaptic functions, and especially collagen and GP6 pathways contributing to ECM may be crucial in the etiology of SCZ. Our rather limited sample size does not allow to make strong conclusions whether astrocytes show sex-specific functional and gene expression differences in SCZ. Nevertheless, our study suggests that such differences may well occur at least in the subset of SCZ patients. Importantly, abnormalities in ECM have been among the strongest findings in iPSC-derived brain cells already in three datasets (Kathuria et al., 2019; Szabo et al., 2021; Tiihonen et al., 2021), highlighting its importance in the pathophysiological process of SCZ. The reproducible results suggest the intriguing possibility that SCZ may be primarily a disease of ECM of the brain: abnormal and insufficient cell adhesion and ECM may result into abnormal neuron guidance and synaptogenesis, leading to imbalance in GABA/glutamate balance, and, finally, to clinical symptoms. Targeting ECM molecules instead of specific neuronal populations may lead to new therapeutic discoveries.

ACKNOWLEDGMENTS

C.R. has been supported by grants from the Academy of Finland (AK 266820) and French National Agency for Research, ANR, Eranet Neuron III program (Acrobat), A.L. by the Academy of Finland (AK 332354). J. Kaprio has been supported by the Academy of Finland (grant 312073). Behavior tests have been performed under Biocenter Finland's funding. J. Koistinaho has been supported by grants from the Academy of Finland (A334525), Sigrid Juselius Foundation and Business Finland. M. Koskuvi has been supported by personal grants from Päijät-Häme Regional Fund, Instrumentarium Science Foundation, and Orion Research Foundation.

AUTHOR CONTRIBUTIONS

Jari Tiihonen and Jari Koistinaho conceived the study. Šárka Lehtonen planned and supervised differentiation of the astrocytes, cell line characterization, sample preparation for RNA sequencing, cell transplantation and histological stainings. Marja Koskuvi differentiated the astrocytes, prepared RNA, FACS, experimental samples, run qRT-PCR, prepared co-cultures for calcium imaging, prepared RNA samples for sequencing and prepared the table for sex-specific DEGs. Kalevi Trontti, Iiris Hovatta performed RNA sequencing analyses and contributed to the interpretation of the results. Tyrone D. Cannon, Jouko Lönnqvist, Sebastian Therman, Jaana Suvisaari, and Jaakko Kaprio gathered the data on twin pairs. Ilkka Ojansuu and Olli Vaurio performed skin biopsies and rating of symptoms. Markku Lähteenvuo contributed to the interpretation of the results. Ida Hyötyläinen grew and differentiated astrocytes and helped in cell preparations. Raisa Giniatullina, Rashid Giniatullin, Jussi Tohka planned calcium-imaging studies together with Marja Koskuvi, Pekka L. J. Virtanen, Anastasia Ludwig and Claudio Rivera who performed the calcium-imaging experiments and Noora Räsänen, Anastasia Ludwig their analysis. Meike Keuters transplanted the cells and together with Hiramani Dhungana perfused and collected tissue samples; Lidiia Plotnikova prepared tissue samples for stainings and Satu Kaipainen prepared for RNA and imaged brain sections. Ying Chieh Wu imaged the whole-section scans and prepared the graphic figures based on them. Heikki Tanila planned and Hennariikka Koivisto performed the behavior tests and statistical analyses; Lidiia Plotnikova helped to perform the

behavior tests. Marja Koskuvi wrote the first draft of the manuscript and prepared the figures and tables with the help of Šárka Lehtonen, Jari Tiihonen and Jari Koistinaho.

DISCLOSURES

The preprint of this manuscript has been posted on BioRxiv: https://doi.org/10.1101/2020.10.23.350413.

The authors declare no competing interests.

DATA AVAILABILITY STATEMENT

Supplementary Data files show raw RNA seq data. All the calcium imaging analysis codes were written in Matlab and are available on request from the authors. The detailed data of mouse behavioral studies are available on request from the authors. The RNA seq data will also be made avalable in a public repository (GEO) after acceptance for publication.

ORCID

Marja Koskuvi https://orcid.org/0000-0002-1646-9992
Šárka Lehtonen https://orcid.org/0000-0002-5055-9414
Meike Keuters https://orcid.org/0000-0003-4216-1024
Noora Räsänen https://orcid.org/0000-0003-4521-4398
Jari Koistinaho https://orcid.org/0000-0001-6559-1153

REFERENCES

Akkouh, I. A., Ueland, T., Hansson, L., Inderhaug, E., Hughes, T., Steen, N. E., Aukrust, P., Andreassen, O. A., Szabo, A., & Djurovic, S. (2020). Decreased IL-1β-induced CCL20 response in human iPSC-astrocytes in schizophrenia: Potential attenuating effects on recruitment of regulatory T cells. *Brain, Behavior, and Immunity*, *87*, 634–644. https://doi.org/10.1016/j.bbi.2020.02.008

Berretta, S. (2012). Extracellular matrix abnormalities in schizophrenia. *Neuropharmacology*, *62*(3), 1584–1597. https://doi.org/10.1016/j.neuropharm.2011.08.010

Cao, M., MacDonald, J. W., Liu, H. L., Weaver, M., Cortes, M., Durosier, L. D., Burns, P., Fecteau, G., Desrochers, A., Schulkin, J., Antonelli, M. C., Bernier, R. A., Dorschner, M., Bammler, T. K., & Frasch, M. G. (2019). A7 nicotinic acetylcholine receptor signaling modulates ovine fetal brain astrocytes transcriptome in response to endotoxin. *Frontiers in Immunology*, *10*, 1063. https://doi.org/10.3389/fimmu.2019.01063

Cardno, A. G., & Gottesman, I. I. (2000). Twin studies of schizophrenia: From bow-and-arrow concordances to star wars mx and functional genomics. *American Journal of Medical Genetics*, *97*(1), 12–17. https://doi.org/10.1002/(SICI)1096-8628(200021)97:1<12::AID-AJMG3>3.0.CO;2-U

Cherlyn, S. Y. T., Woon, P. S., Liu, J. J., Ong, W. Y., Tsai, G. C., & Sim, K. (2010). Genetic association studies of glutamate, GABA and related genes in schizophrenia and bipolar disorder: A decade of advance. *Neuroscience and Biobehavioral Reviews*, *34*(6), 958–977. https://doi.org/10.1016/j.neubiorev.2010.01.002

Davis, J., Eyre, H., Jacka, F. N., Dodd, S., Dean, O., McEwen, S., Debnath, M., McGrath, J., Maes, M., Amminger, P., McGorry, P. D., Pantelis, C., & Berk, M. (2016). A review of vulnerability and risks for schizophrenia: Beyond the two hit hypothesis. *Neuroscience and Biobehavioral Reviews*, *65*, 185–194. https://doi.org/10.1016/j.neubiorev.2016.03.017

de Boni, L., Gasparoni, G., Haubenreich, C., Tierling, S., Schmitt, I., Peitz, M., Koch, P., Walter, J., Wüllner, U., & Brüstle, O. (2018). DNA methylation alterations in iPSC- and hESC-derived neurons: Potential implications for neurological disease modeling. *Clinical Epigenetics*, *10*(1), 13. https://doi.org/10.1186/s13148-018-0440-0

González-Peñas, J., Costas, J., Villamayor, M. J. G., & Xu, B. (2019). Enrichment of rare genetic variants in astrocyte gene enriched co-expression modules altered in postmortem brain samples of schizophrenia. *Neurobiology of Disease*, *121*, 305–314. https://doi.org/10.1016/j.nbd.2018.10.013

Gray, A. L., Hyde, T. M., Deep-Soboslay, A., Kleinman, J. E., & Sodhi, M. S. (2015). Sex differences in glutamate receptor gene expression in major depression and suicide. *Molecular Psychiatry*, *20*(9), 1057–1068. https://doi.org/10.1038/mp.2015.91

Halassa, M. M., Fellin, T., & Haydon, P. G. (2007). The tripartite synapse: Roles for gliotransmission in health and disease. *Trends in Molecular Medicine*, *13*(2), 54–63. https://doi.org/10.1016/j.molmed.2006.12.005

Hert, M., Schreurs, V., Vancampfort, D., & Winkel, R. (2009). Metabolic syndrome in people with schizophrenia: A review. *World Psychiatry*, *8*(1), 15–22. https://doi.org/10.1002/j.2051-5545.2009.tb00199.x

Javitt, D. C., Spencer, K. M., Thaker, G. K., Winterer, G., & Hajós, M. (2008). Neurophysiological biomarkers for drug development in schizophrenia. *Nature Reviews. Drug Discovery*, *7*(1), 68–83. https://doi.org/10.1038/nrd2463

Jonsson, H., Magnusdottir, E., Eggertsson, H. P., Stefansson, O. A., Arnadottir, G. A., Eiriksson, O., Zink, F., Helgason, E. A., Jonsdottir, I., Gylfason, A., Jonasdottir, A., Jonasdottir, A., Beyter, D., Steingrimsdottir, T., Norddahl, G. L., Magnusson, O. T., Masson, G., Halldorsson, B. V., Thorsteinsdottir, U., … Stefansson, K. (2021). Differences between germline genomes of monozygotic twins. *Nature Genetics*, *53*(1), 27–34. https://doi.org/10.1038/s41588-020-00755-1

Kathuria, A., Lopez-Lengowski, K., Watmuff, B., McPhie, D., Cohen, B. M., & Karmacharya, R. (2019). Synaptic deficits in iPSC-derived cortical interneurons in schizophrenia are mediated by NLGN2 and rescued by N-acetylcysteine. *Translational Psychiatry*, *9*(1), 1–13. https://doi.org/10.1038/s41398-019-0660-x

Khandaker, G. M., Cousins, L., Deakin, J., Lennox, B. R., Yolken, R., & Jones, P. B. (2015). Inflammation and immunity in schizophrenia: Implications for pathophysiology and treatment. *The Lancet Psychiatry*, *2*(3), 258–270. https://doi.org/10.1016/S2215-0366(14)00122-9

Kim, J., Grunke, S. D., Levites, Y., Golde, T. E., & Jankowsky, J. L. (2014). Intracerebroventricular viral injection of the neonatal mouse brain for persistent and widespread neuronal transduction. *The Journal of Visualized Experiments*, *15*(91), 51863. https://doi.org/10.3791/51863

Krencik, R., & Zhang, S. (2011). Directed differentiation of functional astroglial subtypes from human pluripotent stem cells. *Nature Protocols*, *6*(11), 1710–1717. https://doi.org/10.1038/nprot.2011.405

Li, R., Ma, X., Wang, G., Yang, J., & Wang, C. (2016). Why sex differences in schizophrenia. *Journal of Translational Neuroscience (Beijing)*, *1*(1), 37–42. https://doi.org/10.3868/j.issn.2096-0689.01.006

Liu, Z., Osipovitch, M., Benraiss, A., Huynh, N. P. T., Foti, R., Bates, J., Chandler-Militello, D., Findling, R. L., Tesar, P. J., Nedergaard, M., Windrem, M. S., & Goldman, S. A. (2019). Dysregulated glial differentiation in schizophrenia may be relieved by suppression of SMAD4- and REST-dependent signaling. *Cell Reports*, *27*(13), 3832–3843.e6. https://doi.org/10.1016/j.celrep.2019.05.088

Mohan, V., Wade, S. D., Sullivan, C. S., Kasten, M. R., Sweetman, C., Stewart, R., Truong, Y., Schachner, M., Manis, P. B., & Maness, P. F. (2019). Close homolog of L1 regulates dendritic spine density in the mouse cerebral cortex through semaphorin 3B. *The Journal of Neuroscience*, *39*(32), 6233–6250. https://doi.org/10.1523/jneurosci.2984-18.2019

Oksanen, M., Hyötyläinen, I., Trontti, K., Rolova, T., Wojciechowski, S., Koskuvi, M., Viitanen, M., Levonen, A. L., Hovatta, I., Roybon, L., Lehtonen, Š., Kanninen, K. M., Hämäläinen, R. H., & Koistinaho, J. (2020). NF-E2-related factor 2 activation boosts antioxidant defenses and ameliorates inflammatory and amyloid properties in human Presenilin-1 mutated alzheimer's disease astrocytes. *Glia*, *68*(3), 589–599. https://doi.org/10.1002/glia.23741

Oksanen, M., Petersen, A. J., Naumenko, N., Puttonen, K., Lehtonen, Š., Gubert Olivé, M., Shakirzyanova, A., Leskelä, S., Sarajärvi, T., Viitanen, M., Rinne, J. O., Hiltunen, M., Haapasalo, A., Giniatullin, R., Tavi, P., Zhang, S. C., Kanninen, K. M., Hämäläinen, R. H., & Koistinaho, J. (2017). PSEN1 mutant iPSC-derived model reveals severe astrocyte pathology in alzheimer's disease. *Stem Cell Reports*, *9*(6), 1885–1897. https://doi.org/10.1016/j.stemcr.2017.10.016

Selemon, L. D., & Zecevic, N. (2015). Schizophrenia: A tale of two critical periods for prefrontal cortical development. *Translational Psychiatry*, *5*(8), e623. https://doi.org/10.1038/tp.2015.115

Skene N. G., Roy M., Grant S. G. N. (2017). A genomic lifespan program that reorganises the young adult brain is targeted in schizophrenia. *eLife*, *6*, e17915. https://doi.org/10.7554/elife.17915

Song, I., & Dityatev, A. (2018). Crosstalk between glia, extracellular matrix and neurons. *Brain Research Bulletin*, *136*, 101–108. https://doi.org/10.1016/j.brainresbull.2017.03.003

Su, J., Chen, J., Lippold, K., Monavarfeshani, A., Carrillo, G. L., Jenkins, R., & Fox, M. A. (2016). Collagen-derived matricryptins promote inhibitory nerve terminal formation in the developing neocortex. *The Journal of Cell Biology*, *212*(6), 721–736. https://doi.org/10.1083/jcb.201509085

Su, J., Cole, J., & Fox, M. A. (2017). Loss of interneuron-derived collagen XIX leads to a reduction in perineuronal nets in the mammalian telencephalon. *ASN Neuro*, *9*(1), 1759091416689020. https://doi.org/10.1177/1759091416689020

Szabo, A., Akkouh, I. A., Vandenberghe, M., Osete, J. R., Hughes, T., Heine, V., Smeland, O. B., Glover, J. C., Andreassen, O. A., & Djurovic, S. (2021). A human iPSC-astroglia neurodevelopmental model reveals divergent transcriptomic patterns in schizophrenia. *Translational Psychiatry*, *11*(1), 554. https://doi.org/10.1038/s41398-021-01681-4

Tiihonen, J., Koskuvi, M., Lähteenvuo, M., Trontti, K., Ojansuu, I., Vaurio, O., Cannon, T. D., Lönnqvist, J., Therman, S., Suvisaari, J., Cheng, L., Tanskanen, A., Taipale, H., Lehtonen, Š., & Koistinaho, J. (2021). Molecular signaling pathways underlying schizophrenia. *Schizophrenia Research*, *232*, 33–41. https://doi.org/10.1016/j.schres.2021.05.011

Tiihonen, J., Koskuvi, M., Storvik, M., Hyötyläinen, I., Gao, Y., Puttonen, K. A., Giniatullina, R., Poguzhelskaya, E., Ojansuu, I., Vaurio, O., Cannon, T. D., Lönnqvist, J., Therman, S., Suvisaari, J., Kaprio, J., Cheng, L., Hill, A. F., Lähteenvuo, M., Tohka, J., … Koistinaho, J. (2019). Sex-specific transcriptional and proteomic signatures in schizophrenia. *Nature Communications*, *10*(1), 3933–3911. https://doi.org/10.1038/s41467-019-11797-3

Toker, L., Mancarci, B. O., Tripathy, S., & Pavlidis, P. (2018). Transcriptomic evidence for alterations in astrocytes and parvalbumin interneurons in subjects with bipolar disorder and schizophrenia. *Biological Psychiatry (1969)*, *84*(11), 787–796. https://doi.org/10.1016/j.biopsych.2018.07.010

Vitale, A. M., Matigian, N. A., Cristino, A. S., Nones, K., Ravishankar, S., Bellette, B., Fan, Y., Wood, S. A., Wolvetang, E., & Mackay-Sim, A. (2017). DNA methylation in schizophrenia in different patient-derived cell types. *NPJ Schizophrenia*, *3*(1), 6. https://doi.org/10.1038/s41537-016-0006-0

Wang, C., Aleksic, B., & Ozaki, N. (2015). Glia-related genes and their contribution to schizophrenia. *Psychiatry and Clinical Neurosciences*, *69*(8), 448–461. https://doi.org/10.1111/pcn.12290

Wen, T. H., Binder, D. K., Ethell, I. M., & Razak, K. A. (2018). The perineuronal 'safety' net? Perineuronal net abnormalities in neurological disorders. *Frontiers in Molecular Neuroscience*, *11*, 270. https://doi.org/10.3389/fnmol.2018.00270

Windrem, M. S., Osipovitch, M., Liu, Z., Bates, J., Chandler-Militello, D., Zou, L., Munir, J., Schanz, S., McCoy, K., Miller, R. H., Wang, S., Nedergaard, M., Findling, R. L., Tesar, P. J., & Goldman, S. A. (2017). Human iPSC glial mouse chimeras reveal glial contributions to schizophrenia. *Cell Stem Cell*, *21*(2), 195–208.e6. https://doi.org/10.1016/j.stem.2017.06.012

SUPPORTING INFORMATION

Additional supporting information may be found in the online version of the article at the publisher's website.

How to cite this article: Koskuvi, M., Lehtonen, Šárka, Trontti, K., Keuters, M., Wu, Y.-C., Koivisto, H., Ludwig, A., Plotnikova, L., Virtanen, P. L. J., Räsänen, N., Kaipainen, S., Hyötyläinen, I., Dhungana, H., Giniatullina, R., Ojansuu, I., Vaurio, O., Cannon, T. D., Lönnqvist, J., Therman, S., … Koistinaho, J. (2022). Contribution of astrocytes to familial risk and clinical manifestation of schizophrenia. *Glia*, *70*(4), 650–660. https://doi.org/10.1002/glia.24131